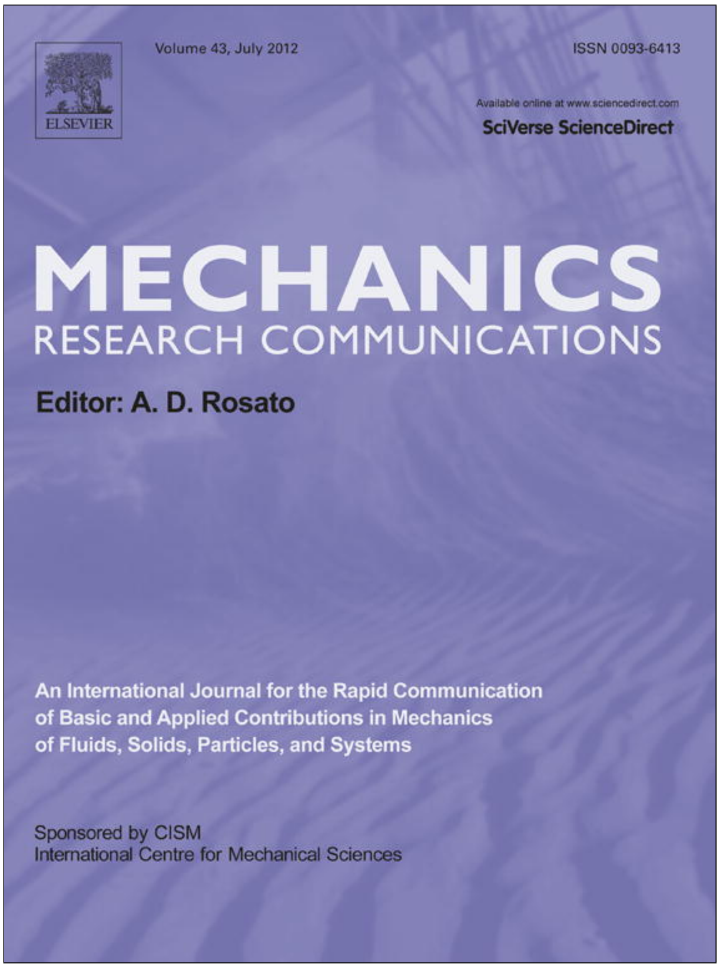
Volume 43, July 2012
ISSN 0093-6413
ELSEVIER
Available online at www.sciencedirect.com
SciVerse ScienceDirect
MECHANICS
RESEARCH COMMUNICATIONS
Editor: A. D. Rosato
An International Journal for the Rapid Communication
of Basic and Applied Contributions in Mechanics
of Fluids, Solids, Particles, and Systems
Sponsored by CISM
International Centre for Mechanical Sciences

Mechanics Research Communications 43 (2012) 46–49

Contents lists available at SciVerse ScienceDirect

Mechanics Research Communications

journal homepage: www.elsevier.com/locate/mechrescom

An analytical model for shear-enhanced adhesiveless transfer printing

Huanyu Cheng[a,1], Jian Wu[b,1], Qingmin Yu[a,c], Hyun-Joon Kim-Lee[d], Andrew Carlson[e], Kevin T. Turner[f], Keh-Chih Hwang[b], Yonggang Huang[a,*], John A. Rogers[e]

[a] Department of Mechanical Engineering and Department of Civil and Environmental Engineering, Northwestern University, Evanston, IL 60208, United States
[b] Department of Engineering Mechanics, Tsinghua University, Beijing 100084, China
[c] School of Mechanics, Civil Engineering and Architecture, Northwestern Polytechnical University, Xi'an 710072, China
[d] Department of Mechanical Engineering, University of Wisconsin, Madison, WI 53706, United States
[e] Department of Materials Science and Engineering, Beckman Institute, and Frederick Seitz Materials Research Laboratory, University of Illinois, Urbana, IL 61801, United States
[f] Department of Mechanical Engineering, University of Pennsylvania, Philadelphia, PA 19104, United States

ARTICLE INFO

Article history:
Received 16 December 2011
Received in revised form 25 February 2012
Accepted 27 February 2012
Available online 8 March 2012

Keywords:
Adhesion
Shear
Transfer printing
Interfacial delamination

ABSTRACT

Transfer printing is an important technique for assembling micro/nanomaterials on unusual substrates, with promising applications in the fabrication of stretchable and flexible electronics designed for use in areas such as biomedicine. The process involves retrieval of structures (e.g., micro-devices) from their growth (donor) substrate via an elastomeric stamp (i.e., an element with posts on its surface), and then delivers them onto a different (receiver) substrate. An analytical mechanics model is developed to identify the key parameters for a shear-enhanced mode for transfer printing. The results predict that the pull-off force decreases linearly with increasing shear strain in the post, or with shear displacement across the stamp. This prediction agrees well with the experiments.

Published by Elsevier Ltd.

Transfer printing is a technique that allows micro-devices to be retrieved (i.e., picked up) from their growth (donor) substrate via an elastomeric stamp, and then allows their delivery onto a different (receiver) substrate (Carlson et al., 2011; Feng et al., 2007; Kim et al., 2009, 2010c; Meitl et al., 2006; Wu et al., 2011). Stretchable electronics represents an application example where transfer printing is critical; the process yields micro-devices printed in arrays onto elastomeric substrates (e.g., PDMS) for systems such as structural health monitoring devices (Nathan et al., 2000), flexible sensors (Lumelsky et al., 2001; Mannsfeld et al., 2010; Someya et al., 2005; Someya and Sekitani, 2009), flexible display (Crawford, 2005; Forrest, 2004; Gelinck et al., 2004), stretchable and foldable circuits (Kim et al., 2008; Sekitani et al., 2010), flexible inorganic solar cells (Yoon et al., 2008) and LEDs (Park et al., 2009; Sekitani et al., 2009). Transfer printing has also been used to develop biomimetic, curvilinear electronics (Ko et al., 2008), bio-dissolvable electronics (Kim et al., 2010a), stretchable and flexible devices for cardiac electrophysiology (Viventi et al., 2010) and ablation therapy (Kim et al., 2011b), foldable electrode array for mapping brain activity (Viventi et al., 2011), smart surgical gloves (Someya et al., 2004), waterproof optoelectronics for biomedicine (Kim et al., 2010b), and epidermal electronics (Kim et al., 2011a).

There exist several different transfer printing techniques.

(1) *Kinetically controlled transfer printing* (Feng et al., 2007; Meitl et al., 2006). The viscoelastic stamp picks up the micro-devices rapidly and prints them slowly onto the receiver substrate because it has high and low adhesion strengths at the large and small peeling rates, respectively.
(2) *Surface-relief-assisted transfer printing* (Kim et al., 2010c; Wu et al., 2011). The stamp surface consists of surface relief structures, such as microtips, to achieve large surface contact with micro-devices (and therefore large adhesion force) during pickup, and small contact area during printing.
(3) *Load-enhanced transfer printing* (Carlson et al., 2011; Kim et al., 2009). Different mechanical loading protocols are adopted to facilitate large and small adhesion forces during pickup and printing, respectively. Directional shearing at an interface is shown to control the behavior in various micro- and nano-structured dry adhesives (Aksak et al., 2008; Jeong et al., 2009; Kramer et al., 2010; Murphy et al., 2009; Varenberg and Gorb, 2007). In particular, shear-enhanced transfer printing (Carlson et al., 2011) shows that the directional shearing at an interface mechanically initiates separation at the adhesive surface and therefore can be used to facilitate the printing of micro-devices.

* Corresponding author.
E-mail address: y-huang@northwestern.edu (Y. Huang).
[1] These authors contributed equally.

0093-6413/$ – see front matter. Published by Elsevier Ltd.
doi:10.1016/j.mechrescom.2012.02.011

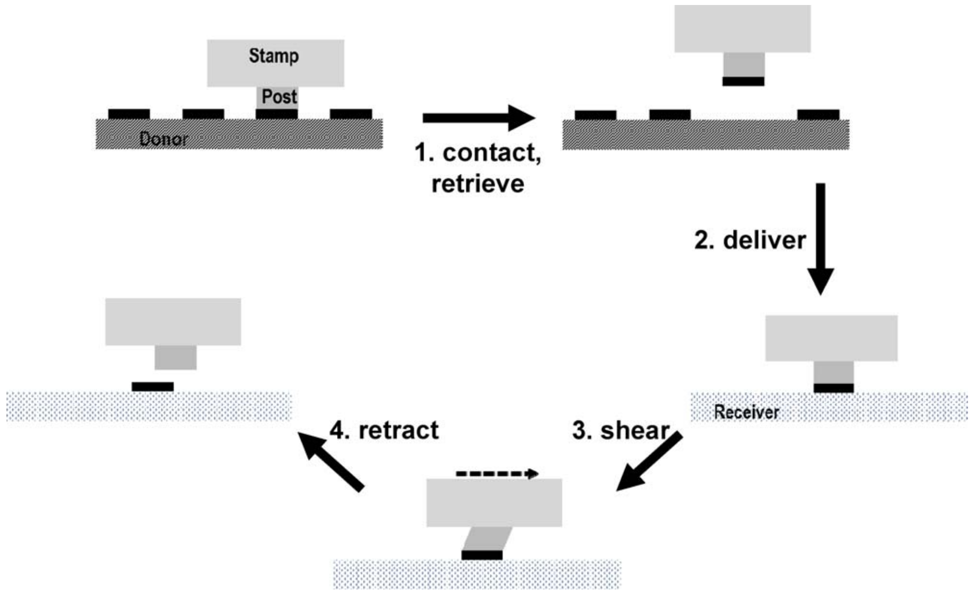

Fig. 1. Illustration of the shear-enhanced transfer printing technique. During pickup, the stamp is retracted rapidly to maximize adhesion after conformal contact to the micro-device. To print, the stamp with micro-device is placed in contact with a receiver substrate, which is displaced laterally followed by a slow retraction on the stamp.

(4) *Laser-driven transfer printing* (Saeidpourazar et al., in press). During printing a laser pulse initiates separation at the adhesive surface due to large thermal mismatch between the stamp and micro-devices.

For kinetically controlled and surface-relief-assisted transfer printing, Feng et al. (2007) and Wu et al. (2011) developed analytical mechanics models to establish the scaling laws, respectively, i.e., a single (or few) non-dimensional combination of key parameters that governs the transfer printing. For shear-enhanced transfer printing, Carlson et al. (2011) developed the numerical model (finite element analysis). A schematic illustration of shear-enhanced transfer printing is shown in Fig. 1. An elastomeric stamp is a single, rectangular post mounted to a thick backing layer. The post and the underlying micro-device to be transferred have identical lateral dimensions, and have conformal contact. The micro-device is picked up rapidly to maximize adhesion through viscoelastic effects of the stamp. The stamp with the micro-device is placed in contact with a receiver substrate. The receiver substrate is then displaced laterally to induce shear on the stamp, which reduces the pull-off force of the stamp to slowly delaminate from the micro-device. The induced shear facilitates the efficient printing of the micro-device onto the receiver substrate.

The purpose of this paper is to establish analytically the scaling law for shear-enhanced transfer printing. Specifically, the reduced pull-off force of the stamp is obtained analytically in terms of the shear strain. This relation is validated by the experiments, and is useful to the optimal design of the stamp for shear-enhanced transfer printing.

Fig. 2 shows a schematic diagram of the stamp and micro-device. On top of a thick backing layer ($H = 950\,\mu$m), the poly(dimethylsiloxane) (PDMS, 5:1 monomer:catalyst mix ratio) post ($L \times L \times h = 100\,\mu\text{m} \times 100\,\mu\text{m} \times 50\,\mu\text{m}$) was brought into intimate contact onto a monocrystalline silicon micro-device ($100\,\mu\text{m} \times 100\,\mu\text{m} \times 3\,\mu\text{m}$) illustrated as a black plate. The backing layer and post are casted and cured together to form the stamp from a prepolymer of PDMS, which ensures strong bonding between the backing layer and post. Using a custom adhesion test setup described elsewhere (Kim et al., 2010c), the shear displacement u was applied on the micro-device in the x direction followed by a vertical retraction with pull-off force F on the stamp in the z direction.

The shear strain in the post γ is determined analytically from the shear displacement u and stamp geometry. The backing layer is much wider and thicker than the post, and is modeled as a semi-infinite solid subjected to a shear stress τ in the x direction over the post area $L \times L$ at the surface of $z = 0$ as shown in Fig. 2. For a concentrated shear force $\tau dx_0 dy_0$ at (x_0,y_0) over an infinitesimal area $dx_0 dy_0$ of the bottom surface, the x-direction displacement at (x,y) on the surface is $dw = \tau dx_0 dy_0 / [2\pi\mu\sqrt{(x-x_0)^2 + (y-y_0)^2}][1 - \nu + \nu((x-x_0)^2/[(x-x_0)^2 + (y-y_0)^2)]]$ (Landau and Lifshitz, 1986), where μ and ν are the shear modulus and Poisson's ratio of the stamp, respectively. For a uniform shear stress τ applied to the post, the displacement at (x,y) is

$$w(x,y) = \int_{L\times L} dw = \frac{\gamma}{2\pi}\int_{-L/2}^{L/2} dx_0 \int_{-L/2}^{L/2} \frac{1}{\sqrt{(x-x_0)^2 + (y-y_0)^2}} \times \left[1 - \nu + \nu\frac{(x-x_0)^2}{(x-x_0)^2 + (y-y_0)^2}\right] dy_0, \tag{1}$$

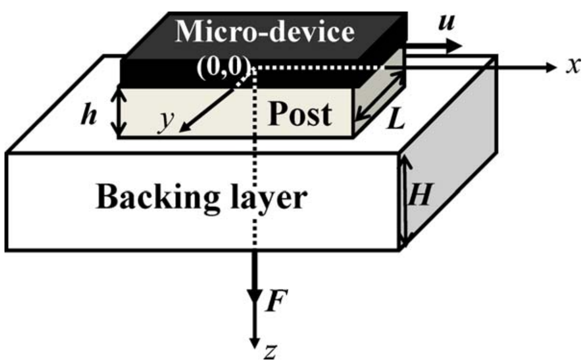

Fig. 2. The critical dimensions of the post and backing layer and loading conditions in a custom adhesion test set up.

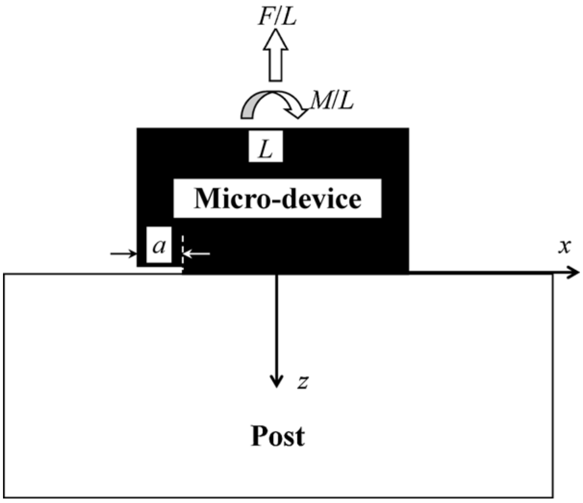

Fig. 3. Schematic illustration of the fracture mechanics model used to study the relationship between vertical pull-off and applied shear in shear-enhanced transfer printing.

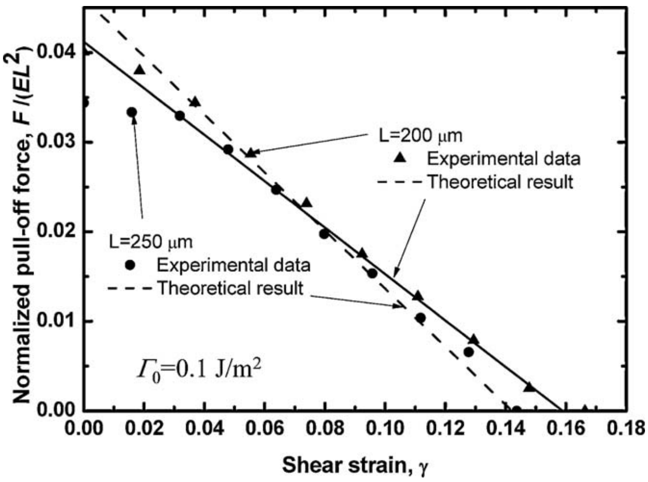

Fig. 4. The normalized pull-off force P as a function of the shear strain γ for post height $h = 50\,\mu$m and post width $L = 200\,\mu$m and $L = 250\,\mu$m. Symbols and lines represent experimental (Carlson et al., 2011) and theoretical results, respectively.

where $\gamma = \tau/\mu$ is the shear strain in the post. The displacement at the origin of the coordinate system $\bar{u}$ along the shear (x) direction is obtained by integrating Eq. (1),

$$\bar{u} = w(0,0) = \frac{2-\nu}{\pi}\gamma L \ln(\sqrt{2}+1). \tag{2}$$

The measured shear displacement u is the sum of $\bar{u}$ and the shear displacement γh across the post, i.e.,

$$u = \bar{u} + \gamma h. \tag{3}$$

Substitution of Eq. (2) into Eq. (3) yields the shear strain in the post,

$$\gamma = \frac{u}{h + ((2-\nu)/\pi)L\ln(\sqrt{2}+1)} \approx \frac{u}{h + (3/2\pi)L\ln(\sqrt{2}+1)}, \tag{4}$$

where the Poisson's ratio $\nu \approx 1/2$ for a PDMS stamp. The above expression has been verified by the finite element method, as described in details by Carlson et al. (2011).

A fracture mechanics model is developed to calculate the pull-off force. Fig. 3 shows an edge crack of length a at the interface between the post and micro-device. The post is subjected to a pull-off force F and shear strain γ. The bending moment that results from the shear stress τ (or shear strain γ) is $M = \tau h L^2 = \mu\gamma h L^2$. The stress intensity factors are obtained analytically as (Tada et al., 2000)

$$K_I = \sqrt{\frac{\pi L}{(1-\lambda)^3}}\left[\frac{F}{L^2}(0.379 + 0.624\lambda - 0.062e^{-12(\lambda/(1-\lambda))}) + \frac{M}{L^3}(2.005 - 0.72e^{-9(\lambda/(1-\lambda))})\right],$$

$$K_{II} = \sqrt{\frac{\pi L}{(1-\lambda)^3}}\left\{\frac{F}{L^2}[0.126 - 0.24\lambda - 0.023(1-\lambda)^5] + \frac{M}{L^3}[-0.228 + (1-\lambda)^4(0.577 - 0.2\lambda + 0.8\lambda^2)]\right\} \tag{5}$$

where $\lambda = a/L$. For an infinitesimal crack, $\lambda \to 0$, the above equation is simplified to

$$K_I = \sqrt{\pi L}\left(0.317\frac{F}{L^2} + 1.285\frac{M}{L^3}\right),$$

$$K_{II} = \sqrt{\pi L}\left(0.103\frac{F}{L^2} + 0.349\frac{M}{L^3}\right). \tag{6}$$

The crack tip energy release rate is given by $G = (K_I^2 + K_{II}^2)/(2\bar{E})$, where the plane-strain modulus of the stamp $\bar{E} \approx 4E/3$, E is the Young's modulus, and the factor 1/2 accounts for the large elastic mismatch between the stamp and micro-device (Huang et al., 2005). The substitution of Eq. (6) into the crack tip energy release rate gives

$$G = \pi E L\left[0.0417\left(\frac{F}{EL^2}\right)^2 + 0.0701\left(\frac{\gamma h}{L}\right)^2 + 0.108\frac{F}{EL^2}\frac{\gamma h}{L}\right]. \tag{7}$$

For the fracture toughness Γ_0 of the stamp/micro-device interface, the Griffith fracture criterion $G = \Gamma_0$ gives the normalized pull-off force

$$\frac{F}{EL^2} = \sqrt{24.0\frac{\Gamma_0}{\pi E L} - 1.72\cdot 10^{-3}\left(\frac{\gamma h}{L}\right)^2} - 1.30\frac{\gamma h}{L}, \tag{8}$$

which has an excellent approximation

$$\frac{F}{EL^2} + \frac{13\gamma h}{10L} \approx 2\sqrt{\frac{6\Gamma_0}{\pi E L}}. \tag{9}$$

As shown in Fig. 4, the pull-off force decreases linearly with the shear strain in the post for the stamp elastic modulus $E = 1.8$ MPa (Kim et al., 2010c), post height $h = 50\,\mu$m and width $L = 200\,\mu$m and $250\,\mu$m in experiments (Carlson et al., 2011). For the fracture toughness of the stamp/micro-device interface $\Gamma_0 = 0.1$ N/m, the pull-off force in Eqs. (8) or (9) agrees well with Carlson et al.'s experiments (2011).

Substitution of the shear strain in Eq. (4) into Eq. (9) gives the pull-off force directly in terms of the shear displacement u as

$$\frac{F}{EL^2} + \frac{u}{L(0.769 + 0.324(L/h))} \approx 2.76\sqrt{\frac{\Gamma_0}{EL}}. \tag{10}$$

The normalized pull-off force $F/(EL^2)$ decreases linearly with the normalized shear displacement u/L, and such a linear dependence depends only the post aspect ratio L/h and normalized interfacial fracture toughness $\Gamma_0/(EL)$.

In general, the interface fracture toughness Γ_0 depends on the mode mixity around an interfacial crack tip. The finite element analysis (Carlson et al., 2011) showed that the phase angle, which represents the mode mixity, is small (~20°) and does not change in the range of applied shear strain in experiments. It is therefore reasonable to use constant fracture toughness in the present analysis.

Eq. (9) also gives the critical shear strain for stamp/micro-device delamination without any pull-off force, $\gamma \approx 2.13\sqrt{\Gamma_0 L/(Eh)^2}$, which agrees well with the experimental data (Carlson et al., 2011) for the vanishing pull-off force. For the other limit of vanishing shear, Eq. (9) gives the pull-off force $F \approx 2.76\sqrt{\Gamma_0 EL^3}$.

In summary, an analytical mechanics model is established for shear-enhanced transfer printing. A simple, analytic equation (9) clearly shows the linear decrease of pull-off force with the increasing shear strain in the post, which agrees well with the experiments.

Acknowledgments

Y.H. and J.A.R. acknowledge support from NSF Grant Nos. CMMI-0749028, ECCS-0824129 and OISE-1043143, and DOE, Division of Materials Sciences Grant No. DE-FG02-07ER46453. H.-J.K. and K.T.T. acknowledge support from AFOSR-MURI FA9550-08-1-0337 and NSF CMMI-0845294.

References

Aksak, B., Murphy, M.P., Sitti, M., 2008. Gecko inspired micro-fibrillar adhesives for wall climbing robots on micro/nanoscale rough surfaces. In: IEEE International Conference on Robotics and Automation, Pasadena, CA, pp. 3058–3063.

Carlson, A., Kim-Lee, H.-J., Wu, J., Elvikis, P., Cheng, H., Kovalsky, A., Elgan, S., Yu, Q., Ferreira, P.M., Huang, Y., Turner, K.T., Rogers, J.A., 2011. Shear-enhanced adhesiveless transfer printing for use in deterministic materials assembly. Applied Physics Letters 98, 264104.

Crawford, G.P., 2005. Flexible Flat Panel Display Technology. Wiley, New York.

Feng, X., Meitl, M.A., Bowen, A.M., Huang, Y., Nuzzo, R.G., Rogers, J.A., 2007. Competing fracture in kinetically controlled transfer printing. Langmuir 23, 12555–12560.

Forrest, S.R., 2004. The path to ubiquitous and low-cost organic electronic appliances on plastic. Nature 428, 911–918.

Gelinck, G.H., Huitema, H.E.A., Van Veenendaal, E., Cantatore, E., Schrijnemakers, L., Van der Putten, J., Geuns, T.C.T., Beenhakkers, M., Giesbers, J.B., Huisman, B.H., Meijer, E.J., Benito, E.M., Touwslager, F.J., Marsman, A.W., Van Rens, B.J.E., De Leeuw, D.M., 2004. Flexible active-matrix displays and shift registers based on solution-processed organic transistors. Nature Materials 3, 106–110.

Huang, Y.G.Y., Zhou, W.X., Hsia, K.J., Menard, E., Park, J.U., Rogers, J.A., Alleyne, A.G., 2005. Stamp collapse in soft lithography. Langmuir 21, 8058–8068.

Jeong, H.E., Lee, J.-K., Kim, H.N., Moon, S.H., Suh, K.Y., 2009. A nontransferring dry adhesive with hierarchical polymer nanohairs. Proceedings of the National Academy of Sciences of the United States of America 106, 5639–5644.

Kim, D.-H., Lu, N., Ma, R., Kim, Y.-S., Kim, R.-H., Wang, S., Wu, J., Won, S.M., Tao, H., Islam, A., Yu, K.J., Kim, T.-i., Chowdhury, R., Ying, M., Xu, L., Li, M., Chung, H.-J., Keum, H., McCormick, M., Liu, P., Zhang, Y.-W., Omenetto, F.G., Huang, Y., Coleman, T., Rogers, J.A., 2011a. Epidermal electronics. Science 333, 838–843.

Kim, D.H., Ahn, J.H., Choi, W.M., Kim, H.S., Kim, T.H., Song, J.Z., Huang, Y.G.Y., Liu, Z.J., Lu, C., Rogers, J.A., 2008. Stretchable and foldable silicon integrated circuits. Science 320, 507–511.

Kim, D.H., Lu, N.S., Ghaffari, R., Kim, Y.S., Lee, S.P., Xu, L.Z., Wu, J.A., Kim, R.H., Song, J.Z., Liu, Z.J., Viventi, J., de Graff, B., Elolampi, B., Mansour, M., Slepian, M.J., Hwang, S., Moss, J.D., Won, S.M., Huang, Y.G., Litt, B., Rogers, J.A., 2011b. Materials for multifunctional balloon catheters with capabilities in cardiac electrophysiological mapping and ablation therapy. Nature Materials 10, 316–323.

Kim, D.H., Viventi, J., Amsden, J.J., Xiao, J.L., Vigeland, L., Kim, Y.S., Blanco, J.A., Panilaitis, B., Frechette, E.S., Contreras, D., Kaplan, D.L., Omenetto, F.G., Huang, Y.G., Hwang, K.C., Zakin, M.R., Litt, B., Rogers, J.A., 2010a. Dissolvable films of silk fibroin for ultrathin conformal bio-integrated electronics. Nature Materials 9, 511–517.

Kim, R.H., Kim, D.H., Xiao, J.L., Kim, B.H., Park, S.I., Panilaitis, B., Ghaffari, R., Yao, J.M., Li, M., Liu, Z.J., Malyarchuk, V., Kim, D.G., Le, A.P., Nuzzo, R.G., Kaplan, D.L., Omenetto, F.G., Huang, Y.G., Kang, Z., Rogers, J.A., 2010b. Waterproof AlInGaP optoelectronics on stretchable substrates with applications in biomedicine and robotics. Nature Materials 9, 929–937.

Kim, S., Wu, J.A., Carlson, A., Jin, S.H., Kovalsky, A., Glass, P., Liu, Z.J., Ahmed, N., Elgan, S.L., Chen, W.Q., Ferreira, P.M., Sitti, M., Huang, Y.G., Rogers, J.A., 2010c. Microstructured elastomeric surfaces with reversible adhesion and examples of their use in deterministic assembly by transfer printing. Proceedings of the National Academy of Sciences of the United States of America 107, 17095–17100.

Kim, T.H., Carlson, A., Ahn, J.H., Won, S.M., Wang, S.D., Huang, Y.G., Rogers, J.A., 2009. Kinetically controlled, adhesiveless transfer printing using microstructured stamps. Applied Physics Letters 94.

Ko, H.C., Stoykovich, M.P., Song, J.Z., Malyarchuk, V., Choi, W.M., Yu, C.J., Geddes, J.B., Xiao, J.L., Wang, S.D., Huang, Y.G., Rogers, J.A., 2008. A hemispherical electronic eye camera based on compressible silicon optoelectronics. Nature 454, 748–753.

Kramer, R.K., Majidi, C., Wood, R.J., 2010. Shear-mode contact splitting for a microtextured elastomer film. Advanced Materials 22, 3700.

Landau, L.D., Lifshitz, E.M., 1986. Theory of Elasticity, 3rd ed. Butterworth Heinemann, Oxford, England.

Lumelsky, V.J., Shur, M.S., Wagner, S., 2001. Sensitive skin. IEEE Sensors Journal 1, 41–51.

Mannsfeld, S.C.B., Tee, B.C.K., Stoltenberg, R.M., Chen, C.V.H.H., Barman, S., Muir, B.V.O., Sokolov, A.N., Reese, C., Bao, Z., 2010. Highly sensitive flexible pressure sensors with microstructured rubber dielectric layers. Nature Materials 9, 859–864.

Meitl, M.A., Zhu, Z.T., Kumar, V., Lee, K.J., Feng, X., Huang, Y.Y., Adesida, I., Nuzzo, R.G., Rogers, J.A., 2006. Transfer printing by kinetic control of adhesion to an elastomeric stamp. Nature Materials 5, 33–38.

Murphy, M., Aksak, B., Sitti, M., 2009. Gecko inspired directional and controllable adhesion. Small 5, 170.

Nathan, A., Park, B., Sazonov, A., Tao, S., Chan, I., Servati, P., Karim, K., Charania, T., Striakhilev, D., Ma, Q., Murthy, R.V.R., 2000. Amorphous silicon detector and thin film transistor technology for large-area imaging of X-rays. Microelectronics Journal 31, 883–891.

Park, S.I., Xiong, Y.J., Kim, R.H., Elvikis, P., Meitl, M., Kim, D.H., Wu, J., Yoon, J., Yu, C.J., Liu, Z.J., Huang, Y.G., Hwang, K., Ferreira, P., Li, X.L., Choquette, K., Rogers, J.A., 2009. Printed Assemblies of Inorganic Light-Emitting Diodes for Deformable and Semitransparent Displays. Science 325, 977–981.

Saeidpourazar, R., Li, R., Li, Y.H., Sangid, M.D., Lu, C.F., Huang, Y., Rogers, J.A., Ferreira, P.M., in press. Laser-driven non-contact transfer printing of prefabricated microstructures. Journal of Microelectromechanical Systems.

Sekitani, T., Nakajima, H., Maeda, H., Fukushima, T., Aida, T., Hata, K., Someya, T., 2009. Stretchable active-matrix organic light-emitting diode display using printable elastic conductors. Nature Materials 8, 494–499.

Sekitani, T., Zschieschang, U., Klauk, H., Someya, T., 2010. Flexible organic transistors and circuits with extreme bending stability. Nature Materials 9, 1015–1022.

Someya, T., Kato, Y., Sekitani, T., Iba, S., Noguchi, Y., Murase, Y., Kawaguchi, H., Sakurai, T., 2005. Conformable, flexible, large-area networks of pressure and thermal sensors with organic transistor active matrixes. Proceedings of the National Academy of Sciences of the United States of America 102, 12321–12325.

Someya, T., Sekitani, T., 2009. Printed skin-like large-area flexible sensors and actuators. In: Brugger, J.B.D. (Ed.), Proceedings of the Eurosensors Xxiii Conference. , pp. 9–12.

Someya, T., Sekitani, T., Iba, S., Kato, Y., Kawaguchi, H., Sakurai, T., 2004. A large-area, flexible pressure sensor matrix with organic field-effect transistors for artificial skin applications. Proceedings of the National Academy of Sciences of the United States of America 101, 9966–9970.

Tada, H., Paris, P.C., Irwin, G.R., 2000. The Stress Analysis of Cracks Handbook, 3rd ed. American Society of Mechanical Engineers, New York.

Varenberg, M., Gorb, S., 2007. Shearing of fibrillar adhesive microstructure: friction and shear-related change in pull-off force. Journal of the Royal Society, Interface 4, 721.

Viventi, J., Kim, D.-H., Vigeland, L., Frechette, E.S., Blanco, J.A., Kim, Y.-S., Avrin, A.E., Tiruvadi, V.R., Hwang, S.-W., Vanleer, A.C., Wulsin, D.F., Davis, K., Gelber, C.E., Palmer, L., Van der Spiegel, J., Wu, J., Xiao, J., Huang, Y., Contreras, D., Rogers, J.A., Litt, B., 2011. Flexible, foldable, actively multiplexed, high-density electrode array for mapping brain activity in vivo. Nature Neuroscience 14, 1599–1605.

Viventi, J., Kim, D.H., Moss, J.D., Kim, Y.S., Blanco, J.A., Annetta, N., Hicks, A., Xiao, J.L., Huang, Y.G., Callans, D.J., Rogers, J.A., Litt, B., 2010. A conformal, bio-interfaced class of silicon electronics for mapping cardiac electrophysiology. Science Translational Medicine 2.

Wu, J., Kim, S., Chen, W., Carlson, A., Hwang, K.-C., Huang, Y., Rogers, J.A., 2011. Mechanics of reversible adhesion. Soft Matter 7, 8657–8662.

Yoon, J., Baca, A.J., Park, S.I., Elvikis, P., Geddes, J.B., Li, L.F., Kim, R.H., Xiao, J.L., Wang, S.D., Kim, T.H., Motala, M.J., Ahn, B.Y., Duoss, E.B., Lewis, J.A., Nuzzo, R.G., Ferreira, P.M., Huang, Y.G., Rockett, A., Rogers, J.A., 2008. Ultrathin silicon solar microcells for semitransparent, mechanically flexible and microconcentrator module designs. Nature Materials 7, 907–915.